

the situation for vacancies. Also, the largest absolute displacement for these far ions is usually less than 3% of the equilibrium lattice spacing. Therefore, the correcting of defect host-lattice ion interactions past first neighbors for lattice relaxation will probably not alter the present values significantly, although again, making anharmonic corrections between first and second neighbors may prove to be worthwhile.

Another possible consideration for future study should be that of properly describing anion-anion deformation dipole interactions, and then allowing these additional dipoles (as well as those from cation-anion deformation) to interact with the elec-

tric field at the NN lattice site. This field should include the contribution from the defect as well as the contributions from the host-lattice ions.

In conclusion, the method of lattice statics together with the deformation dipole model for ionic crystals has given a good description of cation and anion interstitial defects. Our results give confidence that an ion in any interstitial configuration can be properly treated. Thus, the methods and the manner of treating the defect host-lattice ion interactions for both the problem considered here and the study of vacancies should prove to be useful for the study of other defect problems, e. g., vacancy pairs and vacancy migration configurations.

[†]Work performed in part under the auspices of the U. S. AEC at the University of California Lawrence Livermore Laboratory.

*Permanent address: Physics Dept., Abilene Christian College, Abilene, Tex. 79601.

¹Paul D. Schulze and John R. Hardy, *Phys. Rev. B* **5**, 3270 (1972).

²H. M. Evjen, *Phys. Rev.* **39**, 675 (1932).

³J. E. Mayer, *J. Chem. Phys.* **1**, 270 (1933).

⁴F. G. Fumi and M. P. Tosi, *J. Phys. Chem. Solids*

25, 31 (1964).

⁵A more complete listing of the ionic displacements and the dipole moments can be obtained from the authors upon request.

⁶At high temperatures Frenkel defects may become important in ionic conductivity for cases where E_F is relatively low, e.g., E_F^+ in NaCl, NaBr, NaI, KI, and RbI; E_F^- in KF and RbF where the cation has an ionic radius comparable to that of the anion.

Diffusion and Transfer of Optical Excitation in $YF_3 : Yb, Ho$

R. K. Watts* and H. J. Richter

Institut für Angewandte Festkörperphysik der Fraunhofer-Gesellschaft, Freiburg i. Br., Germany

(Received 25 February 1972)

An experimental investigation has been made into the nature of the decay of excited Yb^{3+} donors in the presence of Ho^{3+} acceptors in YF_3 . The results imply that the mechanism of donor-acceptor energy transfer is based on electric dipole-dipole interaction. As the donor concentration is increased, three regimes are traversed: negligible diffusion of excitation among donors, diffusion-limited decay, and rapid diffusion.

I. INTRODUCTION

Recently, there has been considerable interest in rare-earth phosphors which convert infrared radiation into visible light.^{1,2} These phosphors, in general, contain Yb^{3+} , which absorbs infrared radiation in a spectral region from about 0.9 to 1 μm and acts as an energy donor, transferring excitation in two or more sequential steps to an energy acceptor— Er^{3+} , Ho^{3+} , or Tm^{3+} —which accumulates the transferred energy and then emits visible light. Of the various host materials studied YF_3 is found to yield particularly efficient up-conversion phosphors² if the Yb concentration is high and corresponds to 20 mole% YbF_3 or more. A consequence of the high Yb concentration is that

the Yb^{3+} excitation migrates rapidly from donor to donor, effectively averaging the donor's environment of acceptors, and therefore the up-conversion process is well described by rate equations.^{3,4} This averaging, however, masks the nature of the donor-acceptor interaction, and hence it has remained unknown. The purpose of this investigation is to determine the nature of the donor-acceptor interaction for one of these phosphors and to provide insight into the role of donor-donor interactions as exemplified in the diffusion of excitation within the donor system.

Measurements of the decay of donor luminescence were made for several series of phosphors with a range of donor and acceptor concentrations. This technique has been applied in the past to de-

lineate energy-transfer processes in organic and inorganic solids, but the diffusion process has seldom been studied. Recently, Weber⁵ has beautifully demonstrated its importance for europium phosphate glass containing small amounts of chromium.

Ho³⁺ was selected as energy acceptor for this investigation since back transfer of energy from the Ho³⁺ to Yb³⁺ is negligible small.

II. EXPERIMENTAL PROCEDURES

The YF₃ samples were prepared in powder form. High-purity yttrium and rare-earth oxides were first combined for the desired composition. The mixture was dissolved, converted to an oxybate, and finally back to an oxide; from this treatment an oxide with yttrium and rare-earth constituents mixed on an atomic scale results. The mixed oxide was converted to trifluoride in a stream of HF gas at a temperature near 1000 °C.

The excitation source for the luminescence decay measurements was a GaAs:Si diode⁶ with peak emission at 0.95 μm. This source was usually pulsed with a pulse width of 50 μsec. To detect the Yb³⁺ ²F_{5/2} - ²F_{7/2} emission at 1 μm, an RCA 7102 photomultiplier (S-1 photocathode) preceded by two filters, an undoped silicon wafer, and a bandpass filter centered at 1.04 μm with 225-Å half-width, was used. Thus, the relatively weak luminescence of longer wavelength was separated from the intense shorter-wavelength excitation radiation. A boxcar integrator was employed to enhance the signal-to-noise ratio. Radiation trapping in the powder samples was found to be negligible. Decay curves were plotted with an x-y recorder and replotted on semilogarithmic paper. The signal averaging was essential, since in some cases data were taken over an intensity range of three orders of magnitude. Data of only relatively poor quality could be obtained by photographing the photomultiplier output displayed on an oscilloscope, and this method was abandoned. All measurements were made at room temperature.

III. THEORETICAL CONSIDERATIONS

Normally an excited state of an isolated ion decays exponentially with a certain lifetime τ. The rate of decay τ⁻¹ generally contains both radiative and nonradiative components. At sufficiently low donor concentrations, donor-donor interactions can be unimportant compared to donor-acceptor interactions in a system containing both donors and acceptors. (Clustering of ions will be assumed negligible as a simplification throughout.) The theory appropriate to this regime has been developed by several authors,⁷⁻¹⁰ and only the results will be summarized here.

For electric multipolar interactions between donors and acceptors, the donor luminescence intensity as a function of time after a short weak excitation pulse is given by⁹

$$\phi(t) = \phi(0) e^{-t/\tau - \alpha(t/\tau)^{3/s}}, \quad (1)$$

where

$$\alpha = \frac{4}{3} \pi \Gamma(1 - 3/s) N_a R_0^3.$$

s = 6, 8, or 10 for dipole-dipole, quadrupole-dipole, and quadrupole-quadrupole interactions, respectively. N_a is the acceptor concentration in ions/cm³ and R₀ is a critical transfer distance defined so that for a donor-acceptor pair with separation R₀ the probability of transfer to the acceptor is equal to the probability of internal decay of the donor at rate τ⁻¹. The transfer rate for donor-acceptor separation R is CR^{-s}, so that R₀^s = Cτ. C is a constant, independent of R.

For donor-acceptor coupling by the exchange mechanism, the transfer rate has been taken as exponentially decreasing with increasing R. This leads to⁹

$$\phi(t) = \phi(0) e^{-t/\tau - \beta g(\gamma t)}, \quad (2)$$

where

$$g(z) = 6z \sum_{m=0}^{\infty} \frac{(-z)^m}{m!(m+1)^4}.$$

β and γ are constants which, like α above, can be related to microscopic interaction parameters. Both Eqs. (1) and (2) describe decays which show initially a nonexponential character and approach a simple exponential with decay rate τ⁻¹ for long times. The initial fast decay is largely due to donors with acceptors nearby, while the slower portion comes from more nearly isolated donors.

When the donor concentration is increased, donor-donor interactions can become important. At sufficiently high donor concentrations the migration of excitation among the donors can become so rapid that the excitation effectively "sees" an average environment of acceptors about a donor. In this limit the observed donor-acceptor transfer rate becomes proportional to acceptor concentration and a rate-equation description of the process is valid. For the intermediate regime a diffusion equation incorporating a donor-acceptor interaction term must be solved for the excitation. The solution for the case of dipole-dipole donor-acceptor interaction has been obtained by Yokota and Tanimoto¹¹.

$$\phi(t) = \phi(0) \exp \left[-t/\tau - 7.44(at)^{1/2} \times \left(\frac{1 + 10.87x + 15.50x^2}{1 + 8.743x} \right)^{3/4} \right], \quad (3)$$

where

$$x = DC^{-1/3} t^{2/3},$$

D is the diffusion coefficient, and $a = CN_a^2$. For sufficiently small t , Eq. (3) reduces to Eq. (1), with $s = 6$. For large t , an exponential dependence with decay rate $\tau^{-1} + 0.91(4\pi N_a C^{1/4} D^{3/4})$ is predicted. For the system $YF_3: Yb, Ho$, it was possible to make measurements in all of the regimes described above by variation of the donor concentrations. (The measurements are explained in Sec. IV.)

YF_3 has an orthorhombic structure. Each Y site has nine nearest-neighbor fluorines. The lack of inversion symmetry at this site makes forced electric-dipole transitions allowed.

IV. MEASUREMENTS

Yb^{3+} is the energy donor and Ho^{3+} is the energy acceptor. The relevant energy levels are shown in Fig. 1. Each of the $^{2S+1}L_J$ multiplets shown by a horizontal line is split by the crystal field of the YF_3 lattice by a few hundred wave numbers. This splitting was not resolved in the experiments. Since measurements were made at room temperature, the results represent a thermal average over the crystal field components.

Yb^{3+} was excited to the $^2F_{5/2}$ level by a 50- μ sec pulse of 0.95- μ m radiation. The pulse intensity was such that less than one in 10^4 Yb's was excited. An excited Yb can decay in two ways. It can decay internally with decay time $\tau = 1.9$ msec; this lifetime is almost entirely radiative since the $^2F_{5/2} - ^2F_{7/2}$ energy separation amounts to the energy of at least 19 lattice phonons.¹² Or it can transfer nonradiatively to the Ho by the nonresonant process $Yb\ ^2F_{5/2} - ^2F_{7/2}, Ho\ ^5I_8 - ^5I_6$. The excess energy is given to the lattice. Because this energy difference is more than twice the energy of

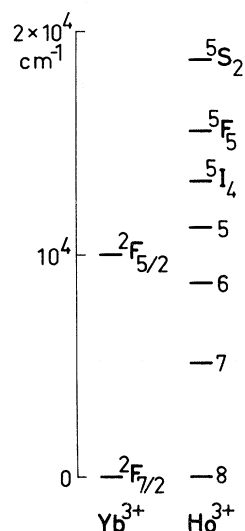


FIG. 1. Energy levels of Yb^{3+} and Ho^{3+} .

an optical phonon,¹³ the transfer is essentially irreversible at room temperature. In the process of infrared to visible conversion the Ho may be further excited from 5I_6 to 5S_2 by a second transfer. Because the fraction of Ho's doubly excited is very small, however, this second step can be ignored for the purposes of this paper. The excitation pulse width should be short enough so that during the pulse the distribution of excitation is unaffected by the acceptors, but long enough to produce useful luminescence intensity. This condition is satisfied for all samples except perhaps $Y_{0.3}Yb_{0.1}Ho_{0.6}F_3$, where better agreement with theory was found by taking the time zero at the middle of the excitation pulse—a shift of 25 μ sec.

Several series of samples $Y_{1-x-y}Yb_xHo_yF_3$ were investigated. x values were 0.001, 0.003, 0.01, 0.03, and 0.1; y values were 0, 0.01, 0.03, 0.06, and 0.1. For $y = 0$, the Yb decay time τ was 1.85 msec at the lowest Yb concentration and was found to decrease to 1.79 msec at the highest Yb concentration, i. e., for $x = 0.1$. This small decrease is probably due to faster diffusion of excitation to Yb's near unintentionally incorporated energy sinks.

V. RESULTS AND DISCUSSION

Examples for the decay of the Yb^{3+} luminescence intensity are shown in Fig. 2–5. At the highest Yb concentrations, exponential decays are observed, and at lower donor concentrations, large initial departures from exponential behavior occur. In order to see which of the possible donor-acceptor interaction mechanisms is effective, one finds that two types of data are of interest: data for the smallest Yb concentrations where donor-donor interactions are smallest, and data showing very large departures from exponentiality at short times where diffusion may not be so important. The curve showing the least exponential character is that for $Y_{0.89}Yb_{0.01}Ho_{0.1}F_3$. The initial part of the decay is shown in Fig. 2, together with fits by Eq. (1) with $s = 6$ and by Eq. (2). The dipole-quadrupole and quadrupole-quadrupole fits are much worse and are omitted for clarity. The dipole-dipole expression fits the data best.

The decays of the samples with $x = 0.001$ and $x = 0.003$, i. e., the decays of the samples with lowest Yb content, are well fitted also by Eq. (1) with $s = 6$. See, for example, Fig. 4. In Fig. 3 the worst of these fits is compared with a fit by the exchange expression [Eq. (2)]. Equation (2) contains two adjustable parameters, β and γ , while Eq. (1) contains only one, α . The dipole-dipole interaction is concluded to be responsible for the donor-acceptor energy transfer.

The other decay curves, e. g., as shown in Fig. 5, can be fitted with Eq. (3). For the curves

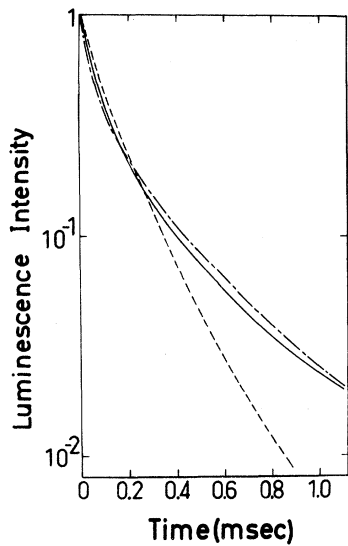


FIG. 2. Initial luminescence decay of Yb^{3+} in $\text{Y}_{0.89}\text{Yb}_{0.01}\text{Ho}_{0.1}\text{F}_3$. The measured curve is solid, the fit with exchange interaction is dashed, and the fit with dipole-dipole interaction is long and short dashed.

showing a large extent of nearly exponential behavior the most reliable values of D are obtained. Conversely, the curves with the greatest departures from an exponential can be expected to yield

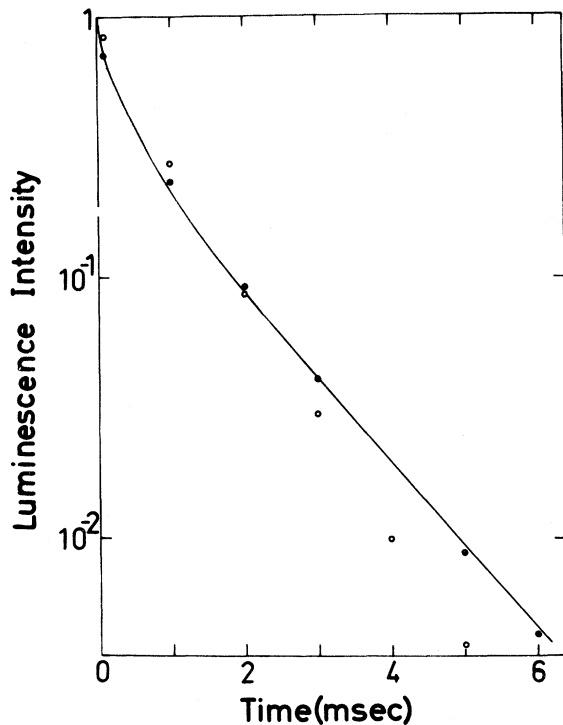


FIG. 3. Luminescence decay of Yb^{3+} in $\text{Y}_{0.937}\text{Yb}_{0.003}\text{Ho}_{0.06}\text{F}_3$. The measured curve is compared with fits by the dipole-dipole interaction (closed circles) and exchange interaction (open circles).

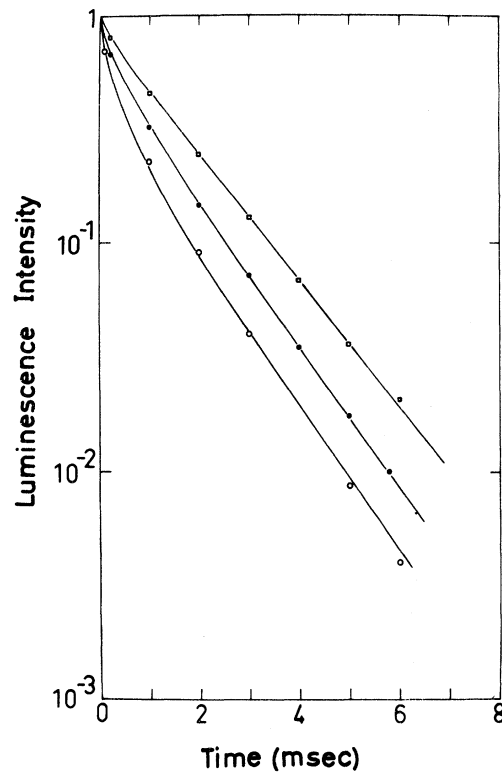


FIG. 4. Luminescence decay of Yb^{3+} in $\text{Y}_{1-x-y}\text{Yb}_x\text{Ho}_y\text{F}_3$. The parameters of the curves are $x=0.003$ and from top to bottom $y=0.01$, $y=0.03$, and $y=0.06$, respectively. The points are fits by Eq. (1) with $s=6$.

the most accurate values of C . The C 's obtained from the fits are shown in Table I. The parameter given by the fits is a . C was calculated from the relation $a = CN_a^2$. a and N_a^2 varied by two orders of magnitude, but the values of C vary by only a factor of 2, if the value for the sample with $x=0.001$, $y=0.06$ is omitted. The average C is $1.8 \times 10^{-41} \text{ cm}^6/\text{sec}$ if this value is included and $2.0 \times 10^{-41} \text{ cm}^6/\text{sec}$ if it is omitted. C will be taken as $2 \times 10^{-41} \text{ cm}^6/\text{sec}$. The value for the critical transfer distance $R_0 = (C\tau)^{1/6}$ thus obtained is 6 \AA . This can be compared with critical separations found for rare earths in calcium metaphosphate glass by Nakazawa and Shionoya¹⁴ ranging from 3 to 12 \AA , depending on the particular donors and

TABLE I. Values of the dipole-dipole coupling parameter C in cm^6/sec for $\text{Y}_{1-x-y}\text{Yb}_x\text{Ho}_y\text{F}_3$.

	$y=0.01$	0.03	0.06	0.1
$x=0.001$	1.6×10^{-41}		4.3×10^{-42}	
0.003	2.2×10^{-41}	1.5×10^{-41}	9.8×10^{-42}	
0.01	1.5×10^{-41}	2.5×10^{-41}	2.3×10^{-41}	3.9×10^{-41}
0.03	1.8×10^{-41}		1.0×10^{-41}	
0.1	2.2×10^{-41}	2.0×10^{-41}	1.8×10^{-41}	

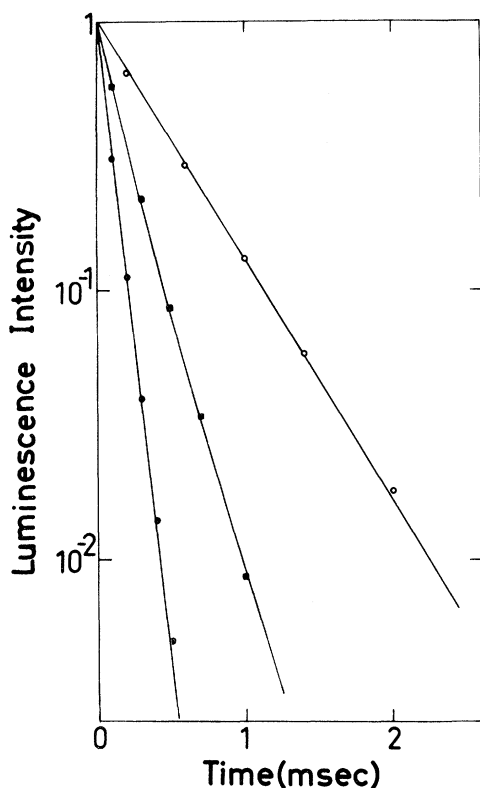


FIG. 5. Luminescence decays of Yb^{3+} in $\text{Y}_{1-x-y}\text{Yb}_x\text{Ho}_y\text{F}_3$. The parameters of the curves are $x=0.1$ and from top to bottom $y=0.01$, $y=0.03$, and $y=0.06$, respectively. For the sample with $y=0.06$, the time zero of the curve has been shifted slightly, as discussed in the text. The points are fits by Eq. (3).

acceptors. For Eu^{3+} donors and Cr^{3+} acceptors in europium phosphate glass, Weber⁵ finds $R_0 = 22 \text{ \AA}$.

Diffusion parameters from fits by Eq. (3) are displayed in Table II. For the two samples with $x=0.01$, $y=0.1$, and $x=0.01$, $y=0.06$ not enough of the asymptotic part of the curves was experimentally available to give reliable values for D . D is seen to be nearly independent of Ho concentration for a given Yb concentration and to increase with increasing Yb concentration as expected. In the concentration range $0.03 \leq x \leq 0.1$, this increase is rather small, which indicates that the

TABLE II. Values of diffusion parameter D in cm^2/sec for $\text{Y}_{1-x-y}\text{Yb}_x\text{Ho}_y\text{F}_3$.

	$y=0.01$	0.03	0.06
$x=0.001$	$< 3 \times 10^{-14}$		$< 3 \times 10^{-14}$
0.003	2.7×10^{-14}	$< 8 \times 10^{-14}$	$< 8 \times 10^{-14}$
0.01	2.9×10^{-12}	1.1×10^{-12}	
0.03	1.1×10^{-11}		1.8×10^{-11}
0.1	1.6×10^{-11}	1.6×10^{-11}	2.2×10^{-11}

TABLE III. Excitation diffusion length $(D\tau)^{1/2}$ compared with the average Yb^{3+} separation $N_d^{-1/3}$ for various Yb concentrations in $\text{Y}_{1-x-y}\text{Yb}_x\text{Ho}_y\text{F}_3$.

x	$(D\tau)^{1/2}$ (in \AA)	$N_d^{-1/3}$ (in \AA)
0.03	17	12
0.01	6	17
0.003	0.8	25

limit of fast diffusion is approached. As the diffusion rate increases, the observed decay rate cannot always continue to increase, since it will eventually be limited by the transfer rate of a donor with an acceptor on a nearest Y site ($\sim 10^4 \text{ sec}^{-1}$). For example, Ostermayer *et al.*¹⁵ find that for a given Tm concentration, the Yb decay rate is the same for $x=0.2$ as for $x=0.1$ in $\text{Y}_{1-x-z}\text{Yb}_x\text{Tm}_z\text{F}_3$. Our largest diffusion parameter $D=2.2 \times 10^{-11} \text{ cm}^2/\text{sec}$ is smaller than the value $D=6 \times 10^{-10} \text{ cm}^2/\text{sec}$ found by Weber for Eu^{3+} excitation in undoped europium phosphate glass. Nakazawa and Shionoya¹⁴ apparently observed no appreciable diffusion in calcium metaphosphate glass at donor concentrations corresponding to $x=0.03$.

For 2 msec, i. e., for the approximate excitation lifetime of Yb^{3+} , the excitation diffusion length $(D\tau)^{1/2}$ is shown in Table III and is compared with the average Yb^{3+} separation. For rare earth in the chlorides Gandrud and Moos¹⁶ find relatively fast diffusion. They report that in 2 msec about 500 and 30 exciton "hops" should occur at donor concentrations corresponding, respectively, to $x=0.03$ and $x=0.01$. If $x=0.03$ there are only 13 Yb's in a sphere of radius 17 \AA [$(D\tau)^{1/2}$ at $x=0.03$ from Table III]; if $x=0.01$, there are two Yb's in a sphere of radius 6 \AA . In these considerations the discrete nature of the lattice has been ignored.

VI. CONCLUSIONS

The importance of excitation diffusion within the donor system has been established for YF_3 : Yb, Ho and, by extension, for other YF_3 phosphors with Yb donors. By variation of the donor concentration it was possible to vary the diffusion coefficient by three orders of magnitude, and three regions were traversed—fast diffusion, diffusion-limited decay, and negligible diffusion. The data are well explained by the dipole-dipole donor acceptor interaction mechanism. The fits to Eq. (3) are internally consistent, as shown in Table I.

ACKNOWLEDGMENTS

We are pleased to acknowledge the generous support of A. Rauber, and we would like to thank H. J. Dietz for preparing the YF_3 samples.

*On leave of absence from Central Research Laboratory, Texas Instruments Inc., Dallas, Tex. 75222.

¹R. A. Hewes and J. F. Sarver, *Phys. Rev.* **182**, 427 (1969).

²J. E. Geusic, F. W. Ostermayer, H. M. Marcos, L. G. Van Uitert, and J. P. van der Ziel, *J. Appl. Phys.* **42**, 1958 (1971).

³J. D. Kingsley, *J. Appl. Phys.* **41**, 175 (1970).

⁴R. K. Watts, *J. Chem. Phys.* **53**, 3552 (1970).

⁵M. J. Weber, *Phys. Rev. B* **4**, 2932 (1971).

⁶Texas Instruments type TIXL 16, fall time 0.2 μ sec.

⁷Th. Förster, *Ann. Physik* **2**, 55 (1948).

⁸D. L. Dexter, *J. Chem. Phys.* **21**, 836 (1953).

⁹M. Inokuti and F. Hirayama, *J. Chem. Phys.* **43**, 1978 (1965).

¹⁰R. Orbach, in *Optical Properties of Ions in Crystals*,

edited by H. M. Crosswhite and H. W. Moos (Interscience, New York, 1967), p. 445.

¹¹M. Yokota and O. Tanimoto, *J. Phys. Soc. Japan* **22**, 779 (1967).

¹²L. A. Riseberg and H. W. Moos, *Phys. Rev.* **174**, 429 (1968).

¹³H. E. Rast, H. H. Caspers, and S. A. Miller, *Phys. Rev.* **180**, 890 (1969).

¹⁴E. Nakazawa and S. Shionoya, *J. Chem. Phys.* **47**, 3211 (1967).

¹⁵F. W. Ostermayer, Jr., J. P. van der Ziel, H. M. Marcos, L. G. Van Uitert, and J. E. Geusic, *Phys. Rev. B* **3**, 2698 (1971).

¹⁶W. B. Gandrud and H. W. Moos, *J. Chem. Phys.* **49**, 2170 (1968).

Crystal Dynamics of Magnesium Oxide

R. K. Singh and K. S. Upadhyaya

Department of Physics, Banaras Hindu University, Varanasi-5, India

(Received 4 October 1971)

The crystal dynamics of magnesium oxide have been studied by incorporating the effect of three-body interactions in the framework of the shell model on the lines of the work of Singh and Verma [*Phys. Rev. B* **2**, 4288 (1970)]. The theoretical dispersion curves in the three symmetry directions and specific-heat variation with temperature have been calculated and compared with the corresponding experimental results. The experimentally observed second-order infrared absorption and the Raman spectra have also been interpreted by using the critical-point analysis and the combined-density-of-states approach. An excellent agreement has been obtained with the recently measured neutron-scattering, specific-heat, and second-order infrared-absorption and Raman-scattering data.

I. INTRODUCTION

In recent years, the availability of the phonon dispersion relations for magnesium oxide by means of the inelastic scattering of thermal neutrons has stimulated considerable interest in the study of its lattice dynamics among both theoretical and experimental workers. It is a solid of great interest and crystallizes in sodium-chloride structure. The studies of the lattice energy and other properties made by Huggins and Sakamoto¹ clearly show that it is purely an ionic solid and its ions Mg and O possess two units of charges (i. e., Mg²⁺ and O²⁻). This material has been found to exhibit a very large deviation from the Cauchy relation ($C_{12} = C_{44}$), C_{44} being approximately twice as large as C_{12} . It has also been observed that the polarizability of the Mg²⁺ is negligibly small as compared to that of O²⁻. Obviously, for a complete investigation of the physical properties of MgO one must use a lattice-dynamical model capable of describing both the elastic and dielectric behavior of ionic solids.

The pioneering work of Kellermann^{2,3} on the dynamics of crystal lattices with NaCl struc-

ture explains the average properties like specific heat well but presents a very poor description of the details of the vibration spectra. The limitations of the theory can be traced to two simplifying assumptions: (a) The ions of the solid are rigid spheres and (b) they interact through central two-body interactions. These assumptions directly lead to the Cauchy relation ($C_{12} = C_{44}$) and fix the value of the high-frequency dielectric constant as unity. Experiments, however, do not support either of these two results, and one is led to believe that the assumptions impose too strong restrictions on the motion of the ions, particularly the outer electronic shells (unpolarizable ions). Thus the rigid-ion model does not take into account the electronic polarization and hence does not include the effect of distortions of the ions due to the lattice waves. A simple presentation of the electronic polarization and distortion effects in ionic crystals is given by an elegant phenomenological theory, which is known as the shell model and has been introduced by Dick and Overhauser⁴ and Hanlon and Lawson.⁵ This model, extended by Woods, Cochran, and Brockhouse⁶ and by Cochran,^{7,8} considers the ions to be